Structural Effects of Framework Mutations on a Humanized Anti-Lysozyme Antibody[1]

Margaret A. Holmes,* Timothy N. Buss,* and Jefferson Foote[2,*,†]

A humanized version of the mouse anti-lysozyme Ab D1.3 was previously constructed as an Fv fragment and its structure was crystallographically determined in the free form and in complex with lysozyme. Here we report five new crystal structures of single-amino acid substitution mutants of the humanized Fv fragment, four of which were determined as Fv-lysozyme complexes. The crystals were isomorphous with the parent forms, and were refined to free *R* values of 28–31% at resolutions of 2.7–2.9 Å. Residue 27 in other Abs has been implicated in stabilizing the conformation of the first complementarity-determining region (CDR) of the H chain, residues 31–35. We find that a Phe-to-Ser mutation at 27 alters the conformation of immediately adjacent residues, but this change is only weakly transmitted to Ag binding residues in the nearby CDR. Residue 71 of the H chain has been proposed to control the relative disposition of H chain CDRs 1 and 2, based on the bulk of its side chain. However, in structures we determined with Val, Ala, or Arg substituted in place of Lys at position 71, no significant change in the conformation of CDRs 1 and 2 was observed. *The Journal of Immunology*, 2001, 167: 296–301.

Humanized Abs are created by replacing the complementarity-determining regions (CDRs)[3] of a human Ab (as defined by Wu and Kabat; Refs. 1, 2) with the corresponding CDRs of a nonhuman Ab (3). This CDR graft transfers the antigenic specificity of the CDR donor molecule, but leaves the new engineered molecule immunologically human, inasmuch as the immunogenicity of humanized Abs in humans is extremely low (4, 5). The first humanized Ab was specific for the hapten nitrophenacetyl. This molecule had been CDR grafted in the H chain only, which was coexpressed with a mouse L chain. The humanized anti-nitrophenacetyl showed 1.5- to 3-fold reduced hapten affinity relative to a control molecule with murine sequences in both chains (3). This finding of altered affinity proved that framework residues can influence the structure of the Ag combining site. Riechmann et al. (4) confirmed this finding in a humanized anti-CD52. The initial humanized construct showed weak avidity. A single Ser-to-Phe mutation at framework residue H27[4] restored avidity to near that of the fully murine control. The importance of framework residues in maintaining the structure of the CDRs and the frequent need for mutational revisions in the framework have since been confirmed many more times during the engineering of humanized Abs to have avidity matching that of their murine antecedents (6).

We developed a humanized anti-lysozyme (HuLys) as a model system for studying structural issues attending the transfer of CDRs from a murine to a human framework (7–9). Thus, murine and human segments for the construction were chosen from among Ab V domains whose structures had been determined. The six CDRs of HuLys come from the murine Ab D1.3, which was raised against hen egg lysozyme (10, 11). The structure of the D1.3 heterodimer of H and L chain V regions (Fv) has been determined at 1.8-Å resolution in both the liganded and unliganded forms (12, 13). The HuLys H chain framework (residues H1–H30, H36–H49, H66–H94, and H103–H113 in the Kabat numbering system) comes from the human myeloma protein NEW, whose structure has been determined at 2.0 Å (14). The κ L chain framework (residues L1–L23, L35–L49, L57–L88, and L98–L108) is a consensus sequence similar to that of the human Bence-Jones protein REI, also determined at 2.0 Å (15).

The crystal structures of the HuLys Fv in free form (16) and complexed with the Ag lysozyme (17) were previously determined at 2.9 and 2.7 Å, respectively (Brookhaven Protein Data Bank accession numbers 1BVL and 1BVK). In this work, we describe crystal structures of a series of single substitution mutants of the HuLys Fv, viz H27S, H71V, H71A, and H71R.

Materials and Methods

Protein engineering

Fvs were expressed in *Escherichia coli* using the pAK19 vector (18), which uses a *phoA* promoter and heat-stable enterotoxin II leader sequence. This vector directs gene products to the periplasm, from which correctly folded, disulfide-oxidized molecules are released after cell harvest. Material used in the present work was released from the periplasm by osmotic shock and purified by affinity chromatography on lysozyme-Sepharose, as described previously (17). Protein concentrations were determined spectrophotometrically, using calculated extinction coefficients (19).

Crystal growth

Crystals of the four mutant complexes were grown in the same way as the native complex crystals (17). Each of the HuLys Fv solutions was mixed with a lysozyme solution in equimolar proportions. The mixtures then sat from several hours to 2 days. PBS was added to dilute the solution, which was centrifuged before use. Protein concentrations ranged from 6.5 to 10.5 mg/ml. The reservoir for vapor diffusion was 0.8 M K_2HPO_4, 0.8 M

*Program in Molecular Medicine, Fred Hutchinson Cancer Research Center, Seattle, WA 98109; and †Department of Immunology, University of Washington, Seattle, WA 98195

Received for publication September 28, 2000. Accepted for publication April 26, 2001.

The costs of publication of this article were defrayed in part by the payment of page charges. This article must therefore be hereby marked *advertisement* in accordance with 18 U.S.C. Section 1734 solely to indicate this fact.

[1] This work was supported by the Department of the Army Breast Cancer Research Program (Grant DAMD 17-97-1-7124).

[2] Address correspondence and reprint requests to Dr. Jefferson Foote, Fred Hutchinson Cancer Research Center, 1100 Fairview Avenue North, C3-168, P.O. Box 19024, Seattle, WA 98109-1024. E-mail address: jfoote@fhcrc.org

[3] Abbreviations used in this paper: CDR, complementarity-determining region; Fv, heterodimer of H and L chain V regions; HuLys, humanized anti-lysozyme; rms, root mean square.

[4] Residues are numbered using the Kabat system and preceded by a chain designator, e.g., H71 for residue 71 in the H chain. The wild-type Fv has Phe at residue H27 and Lys at residue H71; mutant molecules are designated by the substitution, e.g., H71V in an Fv with Val at residue H71.

0022-1767/01/$02.00

Table I. *Data collection*

Structure	H27S Complex	H71V Complex	H71A Complex	H71R Complex	H71V
Space group	$P4_12_12$	$P4_12_12$	$P4_12_12$	$P4_12_12$	$P4_12_12$
Fv/asymmetric unit	2	2	2	2	2
Cell dimensions (Å)	$a=b=97.9$; $c=173.3$	$a=b=96.3$; $c=175.7$	$a=b=97.6$; $c=174.1$	$a=b=97.1$; $c=174.8$	$a=b=146.8$; $c=71.9$
Resolution (Å)	50.0–2.7 2.75–2.70	50.0–2.7 2.75–2.70	50.0–2.7 2.75–2.70	50.0–2.7 2.75–2.70	50.0–2.9 2.95–2.90
Measured reflections	132,637 >2580	141,035 >3001	108,158 >2271	141,201 >2672	88,937 >1849
Unique reflections	23,047 1060	22,318 1133	21,229 1044	22,707 1025	16,618 751
Completeness (%)	96.3 90.3	95.1 97.5	88.9 90.5	95.6 89.0	92.3 87.0
R value[a]	0.065 0.315	0.067 0.404	0.059 0.310	0.065 0.376	0.075 0.403
Average I/σ_I	10.1 2.6	18.1 2.3	17.4 2.6	16.5 2.3	17.2 2.5

[a] $R = \Sigma\Sigma \mid I_{obs} - \langle I_{obs}\rangle \mid / \Sigma\Sigma I_{obs}$.

NaH_2PO_4, 0.1 M HEPES, pH 6.5. Sitting drops consisting of equal volumes of complex solution and reservoir solution were set up in microbridges.

Crystals of the uncomplexed H71V Fv were grown by macroseeding. The seeds were obtained from a hanging drop vapor diffusion crystallization that used 16 mg/ml protein and a reservoir of 0.74 M sodium citrate, 0.01% NaN_3, pH 6.5. Two rounds of seeding were performed. Each time, a few crystals were removed from the drop and placed in a microbridge in a fresh drop composed of equal volumes of Fv solution (16 mg/ml) and reservoir solution (0.8 M sodium citrate, 0.01% NaN_3, pH 6.5).

Data collection

X-ray diffraction data sets were collected from single crystals at 4°C using an R AXIS detector. The data sets were processed with DENZO and SCALEPACK (20, 21). Details of the processing are given in Table I. Before refinement, the data sets were partitioned into a working set and a test set. The test sets for the complexes contained only reflections that had made up the test set for the refinement of the native complex structure, so as to maintain the independence of the test set (22). The test set for the uncomplexed Fv was created by X-PLOR (23), as the refinement of the native Fv structure did not involve a test set.

Refinement

Refinement of the structure of the HuLys H27S Fv-lysozyme complex began with the model of the native complex with residue H27 changed to Gly. A round of rigid body refinement at 3.5-Å resolution was followed by rounds of positional refinement at 2.7-Å resolution using X-PLOR and model building of the loop containing the mutation. A cycle of torsion angle molecular dynamics refinement was run, followed by more rounds of positional refinement and model building. Omit map density was sufficient to model only one of the two H27 side chains. The refinement was completed with a cycle of individual B value refinement with TNT (24) and a cycle of X-PLOR B value refinement. Refinement statistics are given in Table II.

Refinement of the structures of the HuLys H71V, H71A, and H71R Fv-lysozyme complexes was more straightforward. The starting model was the native complex with H71 changed to Gly. A round of rigid body refinement at 3.5-Å resolution was followed by a cycle of positional refinement at 2.7-Å resolution, addition of the H71 side chains to the model, and a second cycle of positional refinement. The refinement was completed with one cycle each of individual B value refinement with TNT and X-PLOR (Table II). Manual changes of the model, other than placement of the H71 side chain, were needed only for the H71A complex.

Refinement of the structure of the uncomplexed HuLys H71V Fv began with H71 changed to Gly. First, a round of rigid body refinement was conducted at 3.5-Å resolution. Next came two rounds of positional refinement at 2.9 Å, alternating with model-building and addition of the H71 side chains. Group B values (1 B per residue) were refined with X-PLOR, and a final cycle of positional refinement was performed (Table II).

No solvent molecules are present in any of the models. PROCHECK (25) analyses of the five structures show no residues in disallowed regions other than L51, which is in a γ-turn conformation, as seen in the native and other related structures (26).

Results

H27S structure

The structure of the HuLys Fv mutant H27S was determined as a lysozyme complex in a crystal form identical with the complex structure obtained previously (17). The crystallographic asymmetric unit contains two Fv:Ag complexes, which we designate molecule 1 and molecule 2. Both Fvs superpose well on the corresponding Fvs of the H27F structure, with root mean square (rms) differences in Cα position of 0.5 Å for each of the two complexes. Despite these identical rms differences, two different conformations are present in the two crystallographically independent H27S molecules. Comparing molecule 1 of H27F and H27S, differences in Cα position of up to 2.7 Å occur at residues H23–H29, adjacent to CDR-H1. The overall effect is that in the H27S structure, this portion of the molecule has moved away from the position of the

Table II. *Refinement*

Parameter	H27S Complex	H71V Complex	H71A Complex	H71R Complex	H71V
Resolution (Å)	10.0–2.7	10.0–2.7	10.0–2.7	10.0–2.7	10.0–2.9
Reflections					
Total (F>2σ)	20,005	19,501	18,592	19,535	14,455
Working set	18,105	17,642	16,805	17,653	13,014
Test set	1,900	1,859	1,787	1,882	1,441
Atoms	5,478	5,486	5,482	5,494	3,484
R value[a]					
Working	0.203	0.202	0.202	0.207	0.225
Free	0.313	0.291	0.291	0.297	0.279
rms deviation from idealityb					
Bond lengths (Å)	0.015	0.014	0.015	0.014	0.021
Bond angles (°)	1.8	1.8	1.9	1.8	2.5
PROCHECK analysis					
% in most favored regions	80.9	81.5	80.5	78.8	78.6
Estimated error in atomic position (Å)c	0.33	0.34	0.33	0.34	0.37

[a] $R = \sum_{hkl} \mid \mid F_{obs_{hkl}} \mid - \mid F_{calc_{hkl}} \mid \mid / \sum_{hkl} \mid F_{obs_{hkl}} \mid$.
[b] Calculated by method of Luzzati (27).

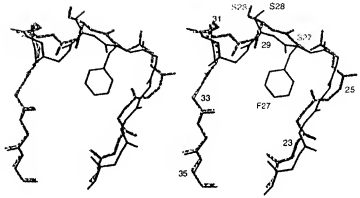

FIGURE 1. Structural effects of different amino acids at position H27, molecule 1. Stereo view of H chain CDR 1 and adjacent peptide segment in H27F (black) and H27S (gray). Atomic coordinates were taken from molecule 1 from the H27F and H27S Fv-lysozyme complex structures. The entire H27S-lysozyme complex was superposed on the H27F-lysozyme complex. The superposed molecules were used for this illustration. Only the peptide backbone from residues H22 to H35 and the side chains from residues H27 and H28 were drawn, to make clear the conformational changes that occur when Ser or Phe is substituted at position H27. Residue H27 in the H27S mutant was modeled as Gly.

Phe side chain present in H27F, toward the H chain N terminus and lysozyme, creating a more open loop (Fig. 1). Residues H74–H76, which pack against CDR-H1, have moved into the space created by this shift. Eight of the Cα shifts larger than twice the rms difference come from residues H23–H29 and H74 and H76. (The others are at chain termini or at locations remote from the combining site.) Modeling of residues H22–H31 was difficult, and the side chain at position H27 could not be fit at all. The possibility exists that this remodeled region is in more than one conformation.

H27S molecule 2 shows a clear difference from the corresponding molecule 2 of the H27F Fv. The Ser and Phe side chains at the substitution site point in opposite directions. As evident in Fig. 2, the phenyl ring of H27F is buried in the interior of the extended loop formed by residues H23–H35, whereas the Ser side chain in H27S points to the aqueous exterior. As predicted (4, 9), substitution of Ser for Phe has created a cavity. Residue Ser H28 in the H27S Fv has shifted so that its main chain and side chain have moved into space occupied by the Phe H27 side chain in the H27F Fv. This large perturbation in backbone conformation extends for several residue positions along the peptide backbone, as is evident in Fig. 2. The shifts of the Cα atoms of residues H23–H31 account for 9 of the 13 shifts greater than twice the rms difference between the mutant and native complexes. A shift at H75 accounts for one more, and the others are at chain termini.

Although the conformation of the loop preceding CDR-H1 differs significantly in H27S and H27F, structural effects on lysozyme binding are small. In the D1.3 complex structure, residue H32 of CDR-H1 makes a weak (3.5 Å) direct contact with lysozyme. Residues H30 and H31 make contact via water molecules (13). In the HuLys H27S structure, the distance for the potential direct contact between H32 and lysozyme is 4.1 Å (molecule 1) or 4.3 Å (molecule 2), similar to the 4.0-Å contact seen in the H27F molecule 1 complex and an increase from the 3.4 Å in the H27F molecule 2 complex, and too large to be important in lysozyme binding (28). Due to the resolution of x-ray data for the HuLys complexes, we have not modeled water molecules, hence we cannot directly compare the Fv-lysozyme interactions involving residues H30 and H31 to the corresponding interactions in D1.3. However, we did compare the positions of the Fv atoms in H27S and H27F involved in these contacts, the carbonyl oxygen atoms of H30 and H31. Both these atoms in H27S molecule 1 have moved 0.8 Å from their positions in H27F. In H27S molecule 2, the backbone Cα atoms of these residues have moved 1.9 Å (H30) and 1.2 Å (H31) from their positions in the H27F complex. The atoms actually forming the contacts, H30 O and H31 O, have moved 1.7 Å and 0.9 Å, respectively. The size of this shift does not necessarily mean that these contacts are broken. The water molecules in the H27S complex presumably could shift position to accommodate the new

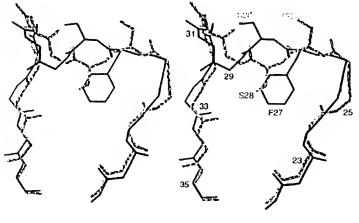

FIGURE 2. Structural effects of different amino acids at position H27, molecule 2. Stereo view of H chain CDR 1 and adjacent peptide segment in H27F (black) and H27S (gray). The illustration was prepared as for Fig. 1, but using atomic coordinates from molecule 2 of the H27F and H27S Fv-lysozyme complex structures.

Table III. *Rms changes in Cα position of H71 mutants relative to H71K*

Mutant	RMS Deviation (Å)	
	Molecule 1	Molecule 2
H71V	0.3	0.3
H71A	0.2	0.2
H71R	0.1	0.1

positions of the protein atoms. The remainder of CDR-H1 in H27S is offset from its location in H27F, with the respective chains back in register by residue H35, the last residue in the CDR.

H71 structures

The size of the side chain at position H71 is thought to control the relative disposition of loops forming CDR-H1 and CDR-H2 (29). Previously published structures of free HuLys Fv and the HuLys-lysozyme complex had Lys in this position. Here we report additional structures with Val, Ala, and Arg at residue H71. All three forms crystallized and were determined as an Fv-lysozyme complex, and a structure of the free H71V Fv was obtained as well.

All the Fv-lysozyme complexes were virtually identical. Superposition of the Cα atoms of the mutant complexes onto the H71K complex gave small rms differences of 0.3 Å or less, as presented in Table III. Twelve Cα atoms in the two H71V molecules have shifts greater than twice the rms differences, and none are near the combining site. Comparing the structures of the H71A and H71K complexes, four Cα atoms have shifts greater than twice the rms difference; three are in the L chain and one is in lysozyme. All are remote from the combining site. The most conservative H71 substitution, arginine for lysine, gave the smallest overall rms difference. However, as for the other H71 mutants, there were moderate shifts of the mutated residue and residues in the nearby segment of polypeptide chain. The Cα atoms of H71 in molecules 1 and 2 moved 0.5 Å and 0.3 Å, respectively, and the preceding Cα atoms in molecule 1, H69 and H70, moved 0.2 Å and 0.4 Å. All other shifts greater than twice the rms distance occurred distant from H71 and from the combining site. Fig. 3 shows superposition of H71 and parts of CDR-H1 and CDR-H2 for the four molecules, taken from the complexed crystal forms. This illustration shows clearly that there is no change in structure of the two CDRs, despite the mutations at H71.

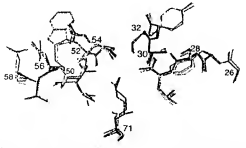

FIGURE 3. Structure of residue H71 and first and second hypervariable loops in four lysozyme-Fv complexes. Conformations of these residues in the two crystallographically independent asymmetric units of all four mutants are essentially identical. This illustration is a composite of superposed molecule 2s seen in H71K (black line), H71V (gray line), H71A (dotted line), and H71R (dashed line). Superpositions were based on H71K molecule 2 and used the Cα atomic coordinates of the residues shown.

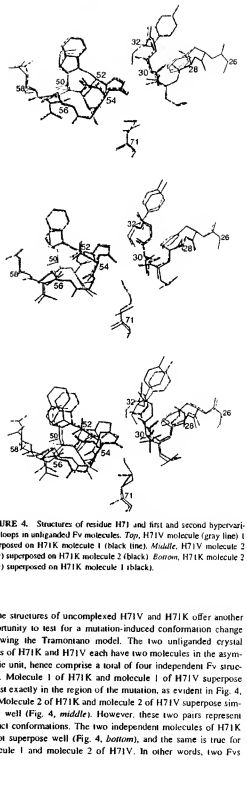

FIGURE 4. Structures of residue H71 and first and second hypervariable loops in unliganded Fv molecules. *Top*, H71V molecule (gray line) superposed on H71K molecule 1 (black line). *Middle*, H71V molecule 2 (gray) superposed on H71K molecule 2 (black). *Bottom*, H71K molecule 2 (gray) superposed on H71K molecule 1 (black).

The structures of uncomplexed H71V and H71K offer another opportunity to test for a mutation-induced conformation change following the Tramontano model. The two unliganded crystal forms of H71K and H71V each have two molecules in the asymmetric unit, hence comprise a total of four independent Fv structures. Molecule 1 of H71K and molecule 1 of H71V superpose almost exactly in the region of the mutation, as evident in Fig. 4, *top*. Molecule 2 of H71K and molecule 2 of H71V superpose similarly well (Fig. 4, *middle*). However, these two pairs represent distinct conformations. The two independent molecules of H71K do not superpose well (Fig. 4, *bottom*), and the same is true for molecule 1 and molecule 2 of H71V. In other words, two Fvs

differing at residue H71, but in identical crystal packing environments, are closer in conformation than two with the same sequence, but in different environments. The two unliganded conformations observed presumably are distinct because of crystal packing interactions, rather than amino acid sequence differences at residue 71. The conformation of H71 and the two loops in the H71K and H71V Fv-lysozyme complexes is intermediate between the two conformations in the unliganded structures, though closer to molecule 2 (rms difference 0.2 Å for the Cα atoms in the illustration superposed on molecule 2 of the H71K complex) than to molecule 1 (0.4 Å rms difference).

Discussion

The role of residues H26–H30 in Ag binding by humanized Abs has been ambiguous. This segment is not considered part of "Kabat" CDR-H1 (residues H31–H35), and these residues rarely contact Ag (30). Other homology- and structure-based definitions of the first Ig H chain CDR have similarly designated residues outside this segment, viz H31–H37 (31), H31–H32 (32), and H30–H35 (33). One exception is the canonical H chain hypervariable loop 1 proposed by Chothia and Lesk (34), extending from H26 to H32. The rationale for this assignment was that the segment forms a loop connecting two β-strands of rather standard geometry. The conservation of particular features in the N-terminal portion of the segment, such as an invariant Gly at position H26, was considered critical for maintaining the backbone conformation of the Ag-contacting C-terminal portion of the H26–H32 loop.

How are conformational changes in CDR-H1 transmitted from the H26–H30 region? Comparison of side-by-side crystal structures of mouse and humanized versions of the same Ab would seem a straightforward way to discover this mechanism, as identical CDR-H1 sequences are abutted in the two cases to H26–H30 regions of separate murine and human origin. However, existing structural data on humanized Abs have been equivocal.

The canonical H26–H32 structure, which the vast majority of Abs adopt (35), is typified by the human H chain NEWM (14, 34). The rat anti-CD52 Ab CAMPATH-1G, with H26–H30 sequence GFTFT, follows this canonical structure precisely (36). The initial humanized form, though based on NEWM frameworks, sequence GSTFS, bound Ag poorly, and probably did not adopt a canonical conformation. The crystallographically studied humanized form, CAMPATH-1H, had higher affinity by virtue of the H26–H30 region being reverted to the rat sequence. Nevertheless, this structure still differed from the canonical conformation at residues H29 and H30. This deviation was attributed to a different interaction with respective side chains at position H71 (Arg in CAMPATH-1G, Val in CAMPATH-1H). A recent structure of the same humanized molecule in complex with an Ag mimotope showed that the H26–H32 loop was once again in the canonical conformation (37).

CDR-H1 of the murine anti-γ-IFN Ab AF2 deviates in conformation from the canonical structure at each position, but is still topologically recognizable as a loop (38). In contrast, the humanized version of AF2, despite having an identical sequence from residue H19–H66, has an α-helical CDR-H1 not seen in any other Ab structure. This unique conformation was attributed to a second structural rearrangement in framework 1 associated with a Pro (mouse) to Ser (humanized) mutation at position H7.

The murine anti-lysozyme Ab D1.3 has a canonical CDR-H1 structure (11). The humanized version of D1.3 whose structure we previously reported (16, 17) has an identical sequence from H26–H35 (7) (H26–H30 sequence GFSLT) and also adopts a canonical CDR-H1 conformation. A kinetic study of HuLys mutants showed that a Ser substitution at residue H27 had only a slightly detrimental effect on Ag affinity (9). This observation was contrary to the profound effect of a Ser-to-Phe mutation in CAMPATH-1H, even though both HuLys and CAMPATH-1H used NEWM framework sequences (4). One possible explanation is that the mutation in HuLys caused no significant structural change. The finding that CDR-H1 of D1.3 contributes little free energy toward lysozyme binding (39) makes plausible an alternative possibility, that the mutation did cause a change in residues H26–H30, but this perturbation was not detectable by kinetic analysis. Crystallographic data presented here favor the latter proposition, made clear in Fig. 1. The HuLys H27S structure shows large changes in backbone conformation in residues H22–H30 in molecule 1 and H26–H30 in molecule 2, but these torsional changes are not transmitted to the nearby Ag binding residues H31 and H32. Translational changes are also not transmitted to these residues, except for a displacement of H31 in molecule 2. Given our findings and the apparent idiosyncrasies observed in other humanized Ab structures, we can only conclude that the conformation of CDR-H1 and the adjacent H26–H30 region are extremely sensitive both to their own sequences and to interactions with adjacent residues. Our understanding of structural determinants of H26–H35 and our ability to rationally manipulate this region remain limited.

Tramontano et al. (29) have articulated a descriptive and predictive model for the structures of the H chain hypervariable loops 1 (Kabat residues H26–H32) and 2 (Kabat residues H52a/53–H55). In this model, the most important determinants of the conformation of hypervariable loop 2 are the length of the loop and specific sequence constraints, with particular canonical structures and conserved residues expected for 3, 4, and 6 residue loops. A further structural determinant is the side chain of residue H71, which is significant in the following way. The position of hypervariable loop 1 is essentially fixed. The position of loop 2 relative to loop 1 is variable, and depends on whether a large side chain at H71 packs between the two loops and separates them or a small side chain at H71 allows loops 1 and 2 to juxtapose.

In HuLys crystal structures with four different side chains at residue H71, the expected conformational rearrangement of the hypervariable loop 2 region is not observed. The absence of a mutation-induced conformation change cannot simply be due to the stabilizing effect of a bound Ag, because the Lys-to-Val mutation in the unliganded crystal forms also does not alter the position of loop 2. The modest (0.4–0.6 kcal/mol) improvement in affinity that accompanied this mutation thus cannot be attributed to relieving an inappropriate displacement of hypervariable loop 2 (9). Our findings do not invalidate the Tramontano model, for which other proof exists, including a specific mutational study of residue H71 in the crystallographically determined Ab B72.3 (40). Our data do demonstrate that a class of exceptions may exist in which the H71 side chain alone does not affect the separation of hypervariable loops 1 and 2. An unknown sequence determinant may override the action of H71, or the compact nature of 3-residue hypervariable loops (H53–H55) may confer less sensitivity to the bulk of the H71 side chain.

The observation that significant conformational changes in the H27S mutant did not lead to much change in Ag affinity, whereas substitutions at H71 gave affinity differences, but no apparent explacatory change in structure illustrates the value of combining structural and kinetic studies.

References

1. Wu, T. T., and E. A. Kabat. 1970. An analysis of the sequences of the variable regions of Bence Jones proteins and myeloma light chains and their implications for antibody complementarity. *J. Exp. Med. 132:211.*
2. Kabat, E. A., T. T. Wu, H. M. Perry, K. S. Gottesman, and K. Coeller. 1991. *Sequences of Proteins of Immunological Interest, 5th Ed.* U.S. Department of

Health and Human Services, Public Health Service, National Institutes of Health, Bethesda, MD

3. Jones, P. T., P. H. Dear, J. Foote, M. S. Neuberger, and G. Winter. 1986. Replacing the complementarity-determining regions in a human antibody with those from a mouse. *Nature 321:522.*
4. Riechmann, L., M. Clark, H. Waldmann, and G. Winter. 1988. Reshaping human antibodies for therapy. *Nature 332:323.*
5. Stephens, S. S. Emtage, O. Vetterlein, L. Chaplin, C. Bebbington, A. Nesbitt, M. Sopwith, D. Athwal, C. Novak, and M. Bodmer. 1995. Comprehensive pharmacokinetics of a humanized antibody and analysis of residual anti-idiotypic responses. *Immunology 85:668.*
6. Winter, G., and W. J. Harris. 1993. Humanized antibodies. *Immunol. Today 14:243.*
7. Verhoeyen, M. E., C. Milstein, and G. Winter. 1988. Reshaping human antibodies: grafting an antilysozyme activity. *Science 239:1534.*
8. Riechmann, L., J. Foote, and G. Winter. 1988. Expression of an antibody Fv fragment in myeloma cells. *J. Mol. Biol. 203:825.*
9. Foote, J., and G. Winter. 1992. Antibody residues affecting conformation of the hypervariable loops. *J. Mol. Biol. 224:487.*
10. Marquart, R. A., D. L. Jenkoski, G. Boulos, A. G. Amit, P. Saludjian, A. Le Guern, J. C. Mazie, and R. J. Poljak. 1983. Preliminary crystallographic study of the complex between the Fab fragment of a monoclonal anti-lysozyme antibody and its antigen. *J. Mol. Biol. 170:1055.*
11. Amit, A. G., R. A. Mariuzza, S. E. V. Phillips, and R. J. Poljak. 1986. Three-dimensional structure of an antigen-antibody complex at 2.8 Å resolution. *Science 233:747.*
12. Bhat, T. N., G. A. Bentley, T. O. Fischmann, G. Boulot, and R. J. Poljak. 1990. Small rearrangements in structures of Fv and Fab fragments of antibody D1.3 on antigen binding. *Nature 347:483.*
13. Bhat, T. N., G. A. Bentley, G. Boulot, M. I. Green, D. Tello, W. Dall'Acqua, H Souchon, F P Schwarz, R. A. Mariuzza, and R. J Poljak. 1994. Bound water molecules and conformational stabilization help mediate an antigen-antibody association. *Proc. Natl Acad. Sci. USA 91:1089.*
14. Saul, F. A., and R. J Poljak. 1992. Crystal structure of human immunoglobulin fragment Fab New refined at 2.0 Å resolution. *Proteins 14:363.*
15. Epp, O., E E Lattman, M Schiffer, R. Huber, and W. Palm. 1975. The molecular structure of a dimer composed of the variable portions of the Bence-Jones protein REI refined at 2.0 Å resolution. *Biochemistry 14:4943.*
16. Holmes, M. A., and J. Foote. 1997. Structural consequences of humanizing an antibody. *J. Immunol. 158:2192.*
17. Holmes, M. A., T. N. Buss, and J. Foote. 1998. Conformational correction mechanisms aiding antigen recognition by a humanized antibody. *J. Exp. Med. 187:479.*
18. Carter, P., R F. Kelley, M. L. Rodrigues, B. Snedecor, M. Covarrubias, M. D. Velligan, W. L. T. Wong, A. M. Rowland, C. E. Kotts, M. E. Carver, et al. 1992. High level *Escherichia coli* expression and production of a bivalent humanized antibody fragment. *BioTechnology (NY) 10:163.*
19. Perkins, S. J. 1986. Protein volumes and hydration effects. *Eur. J. Biochem. 157:169.*
20. Otwinowski, Z. 1993. Oscillation data reduction program. In *Proceedings of the CCP4 Study Weekend: Data Collection and Processing, January 29–30.* L. Sawyer, N. Isaacs, and S. Bailey, eds. SERC Daresbury Laboratory, Warrington, U.K. pp. 56
21. Otwinowski, Z., and W. Minor. 1997. Processing of x-ray diffraction data collected in oscillation mode. *Methods Enzymol. 276:307*
22. Kleywegt, G. J., and A. T. Brünger 1996. Checking your imaginations: applications of the free R value. *Structure 4:897*
23. Brünger, A. T. 1992. *X-PLOR Manual, Version 3.1.* Yale University Press, New Haven, CT.
24. Tronrud, D. E., E. F TenEyck, and B. W Matthews. 1987. An efficient general-purpose least-squares refinement program for macromolecular structures. *Acta Crystallogr. A42:490.*
25. Laskowski, R. A., M. W. MacArthur, D. S. Moss, and J. M. Thornton. 1993. PROCHECK: a program to check the stereochemistry of protein structures. *J. Appl. Crystallogr. 26:283*
26. Maher-White, E. J., B. M. Ross, R. Ismail, K. Belhadj-Mostefa, and R. Poel. 1988. One type of γ-turn, rather than the other gives rise to chain-reversal in proteins. *J. Mol. Biol. 204:777.*
27. Luzzati, V. 1952. Traitment statistique des erreurs dans la determination des structures cristallines. *Acta Crystallogr. 5:802.*
28. Baker, E. N., and R. E. Hubbard. 1984. Hydrogen bonding in globular proteins. *Prog. Biophys. Mol. Biol. 44:97.*
29. Tramontano, A., C. Chothia, and A. M. Lesk 1990. Framework residue 71 is a major determinant of the position and conformation of the second hypervariable region in the V_H domain of immunoglobulins. *J. Mol. Biol. 215:175.*
30. Padlan, E. O., C. Abergel, and J. P. Tipper. 1995. Identification of specificity-determining residues in antibodies. *FASEB J. 9:133.*
31. Capra, J. D. 1971. Hypervariable region of human immunoglobulin heavy chains. *Nat. New Biol. 230:61.*
32. Novotny, J., R. Bruccoleri, J. Newell, D. Murphy, E. Haber, and M. Karplus. 1983. Molecular anatomy of the antibody binding site. *J Biol. Chem. 258:14433.*
33. MacCallum, R. M., A. C. R. Martin, and J. M. Thornton. 1996. Antibody-antigen interactions: contact analysis and binding site topography. *J. Mol. Biol. 262:732*
34. Chothia, C., and A. M. Lesk. 1987. Canonical structures for the hypervariable regions of immunoglobulins. *J. Mol. Biol. 96:901.*
35. Chothia, C., A. M. Lesk, E. Gherardi, I. M. Tomlinson, G. Walter, J. D. Marks, M. B. Llewelyn, and G. Winter. 1992. Structural repertoire of the human V_H segments. *J. Mol. Biol. 227:799.*
36. Chothian, G. M. T., C. Hale, H. Waldmann, and A. C. Bloomer. 1998. Crystal structures of a rat anti-CD52 (CAMPATH-1) therapeutic antibody Fab fragment and its humanized counterpart. *J. Mol. Biol. 284:85.*
37. James, L. C., G. Hale, H. Waldmann, and A. C. Bloomer 1999. 1.9 Å structure of the therapeutic antibody CAMPATH-1H Fab in complex with a synthetic peptide antigen. *J. Mol. Biol. 289:293*
38. Fan, Z. C., L. Shan, B. Z. Goldsteen, L. W. Guddat, A. Thakur, N. F. Landolfi, M. S. Co, M. Vasquez, C. Queen, P. A. Ramsland, and A. B. Edmundson. 1999. Comparison of the three-dimensional structures of a humanized and a chimeric Fab of an anti-γ-interferon antibody. *J. Mol. Recognit. 12:19*
39. Dall'Acqua, W., E. R. Goldman, E. Eisenstein, and R. A. Mariuzza. 1996. A mutational analysis of the binding of two different proteins to the same antibody. *Biochemistry 35:9667.*
40. Xiang, J., Y. Shi, Z. Jin, L. Prasad, and L. T. J. Delbaere 1995. Framework residues 71 and 93 of the chimeric B72.3 antibody are major determinants of the conformation of heavy-chain hypervariable loops. *J. Mol. Biol. 253:385*